

Flow-based CABG patency evaluation: physical and statistical background

Sita Drost, Cornelis J. Drost

1. Introduction

Transit time flow measurement (TTFM) is increasingly used in coronary artery bypass graft (CABG) surgery for the intraoperative evaluation of newly created grafts [1-9]. Deviations in the measured flow waveform can alert the surgeon of possible technical imperfections in the graft before the patient's chest is closed. Presently in Japan, all CABG procedures include some form of flow-based patency assessment [10], while in the United States this percentage lies around 20% [6], the majority of which concerns off-pump CABG surgery. Also, the 2018 ESC/EACTS Guidelines on Myocardial Revascularization [11] recommend TTFM to confirm graft patency.

Flow-based patency evaluation is complicated by the many factors influencing the coronary flow waveform. Myocardial perfusion differs from the flow in the rest of the cardiovascular system in that intramyocardial vessels are highly influenced by their active environment: the contracting wall of the heart. This results in the distinctive diastolic dominant flow rate waveform in coronary arteries [12, 13]. Being anastomosed onto a coronary artery, a CABG graft inherits this diastolic dominant flow waveform. Factors that influence the CABG flow waveform are target coronary, graft type (e.g. arterial or venous, single or sequential), competitive flow (resulting from incomplete occlusion of native coronary), autoregulation, quality of coronary microvasculature (resistance, compliance), but also heart rate, cardiac index, blood pressure, and BMI [14].

Because of the complex nature of CABG surgery, interpreting the measured flow waveform can be challenging. This technical note aims to give the reader a basic understanding of the mechanics, fluid dynamics, and physiology underlying TTFM-based patency metrics. Also, a brief explanation is given of the statistical methods used to evaluate the performance of patency metrics.

2. Coronary Hemodynamics

As already mentioned briefly in the introduction, the coronary flow waveform differs from the flow in the rest of the cardiovascular system because of the influence of the contracting wall of the heart. As illustrated in Figure 1, left and right ventricular contraction cause a rise in systemic and pulmonary pressure, respectively, driving blood circulation. However, this contraction also compresses the myocardial wall, resulting in high intramyocardial pressure, which impedes coronary arterial flow during systole. During diastole, the myocardial wall expands and intramyocardial pressure decreases, leading to increased flow in the coronary arteries. The overall result is the distinctive diastolic dominant flow waveform that is typically observed in coronary arteries. Because the left ventricle contracts more strongly than the right ventricle, diastolic dominance is more pronounced in left coronaries.

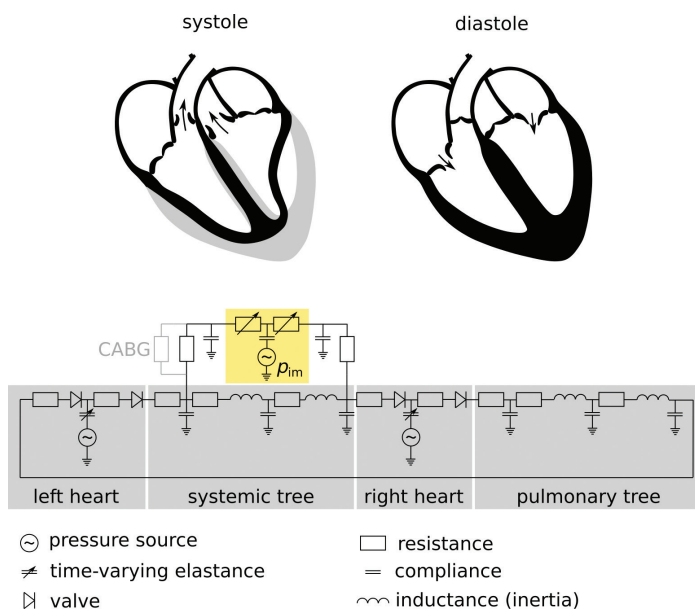


Figure 1. Top: Contraction of the ventricles during systole causes arterial pressure to rise, but also compresses the myocardial wall, resulting in high intramyocardial pressure (p_{im}) and coronary flow impediment. During diastole the myocardium expands and p_{im} decreases. Bottom: Simplified electrical circuit model of human circulation, based on Mantero et al. [15], to illustrate Spaan's intramyocardial pump principle [12] (highlighted in yellow). CABG graft (resistance + compliance) is colored gray to indicate that it is not always present. Ventricles are represented as a combination of a pressure source and a time-varying elastance; p_{im} is represented as a separate source for clarity but originates from ventricular contraction. The action of p_{im} causes volume to be squeezed out of the intramyocardial bed during systole, resulting in low arterial and high venous flow rates. During diastole this effect is reversed, resulting in the typical diastolic dominant coronary flow waveform.

transonic
THE MEASURE OF BETTER RESULTS.

www.transonic.com

Flow-based CABG patency evaluation:

On the venous side, compression of the myocardial wall is the dominant driving force for flow, so that the coronary arterial and venous flow waveforms are in anti-phase [12].

Because a CABG is anastomosed onto a coronary artery, it also experiences the effects of myocardial contraction. Therefore, the flow waveform in a patent graft should display a diastolic dominant pattern similar to its target artery. However, it should be noted that the perfusion pressure waveform in arterial grafts, such as LITA or GEA grafts, differs from the pressure waveform in the ascending aorta, where the coronary ostia are located. Its onset is delayed, and its diastolic and mean pressure are lower [16], resulting in a slightly different flow waveform. Venous grafts generally have their proximal anastomosis on the aortic root, and hence have a perfusion waveform that is virtually indistinguishable from that in (proximal) coronary arteries.

2.1 Stenosis

Blood flow is driven by a pressure gradient and restricted by resistance. A higher pressure gradient leads to a higher flow rate, whereas a higher resistance reduces the flow rate. If a blood vessel becomes constricted, several things happen to the flow (Figure 2). At the site of the constriction, the reduction in diameter causes an increase in flow resistance. This results in an increased pressure drop across the constriction and, in severe cases, turbulence on the distal side (which, in combination with the acceleration and deceleration through the constriction, increases the pressure drop even further) [12, 17]. In the coronary circulation, the reduced pressure distal to a constriction also causes the diameter of the vessels in the intramyocardial vascular bed to decrease, resulting in increased resistance there as well [12]. Because compliance is higher in the subendocardium than in the subepicardium, the diameter decrease and resistance increase are larger in the former, resulting in a reduced endo/epi flow ratio [12, 13]. As subepicardial flow suffers less from systolic flow impediment than subendocardial flow, this reduction of endo/epi flow ratio leads to a decrease in diastolic dominance. Additionally, pressure drop over a constriction depends on flow rate [17], so that the increase in intramyocardial resistance is larger during diastole (high flow rate) than during systole (low flow rate), which further reduces diastolic dominance. Finally, the increase in intramyocardial resistance may (in part) be compensated by autoregulation.

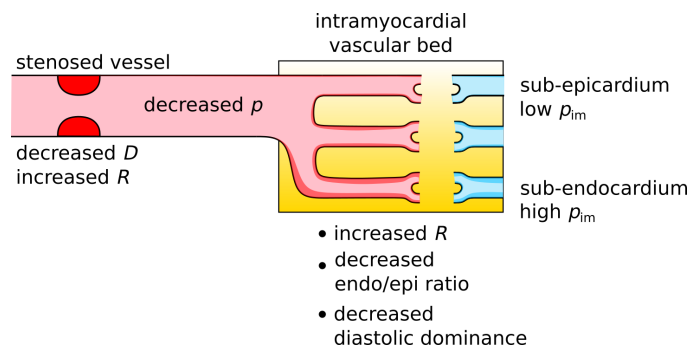


Figure 2. Effects of stenosis: 1. Local: decreased diameter results in increased resistance and lower pressure distal to stenosis. 2. Distal: decreased pressure causes decreased vessel diameter and hence higher resistance in the intramyocardial vascular bed, resulting in decreased endo/epi flow ratio. As subepicardial flow suffers less from systolic flow impediment than subendocardial flow, decreased endo/epi ratio results in decreased diastolic dominance. 3. Dynamical: Pressure drop over stenosis depends on flow rate [17], so effect 2. is stronger during diastole (high flow rate) than during systole (low flow rate).

2.2 Existing TTFM-based Metrics

Box 1: Existing patency metrics

| | |
|-------------------------------|---|
| Mean flow rate: | $Q_{av} = \frac{1}{T} \int_0^T Q(t)dt,$ |
| Pulsatility index: | $PI = \frac{Q_{max} - Q_{min}}{Q_{av}},$ |
| Diastolic filling percentage: | $DF\% = 100 \times \frac{V_{dia}}{V_{tot}},$ |
| Diastolic/systolic ratio: | $D/S\text{-ratio} = \frac{V_{dia}}{V_{sys}}.$ |

physical & statistical background cont.

Flow-based patency metrics quantify one or more of the aspects outlined in the previous subsection. At present, TTFM flow monitors used for intraoperative CABG patency assessment display a selection of metrics (Box 1; see Abbreviations for meaning of variables). If one or more metrics exceed a critical value, the surgeon is prompted to check the newly created graft for technical imperfections, such as twists, kinks, or misapplied stitches (Box 2). As also pointed out by Akhrass and Bakaeen [1], suboptimal metric values should not automatically lead to graft revision; TTFM is intended as a supportive tool, subordinate to the surgeon's expert judgment.

Box 2: Intraoperative TTFM graft patency evaluation protocol

Flow probe: Match graft diameter, avoid graft constriction/compression

Timing: After distal anastomosis completion, preferably with native coronary snared (eliminates any competitive flow)

Position: ± 1 cm proximal to distal anastomosis (too far from anastomosis: compliance artifacts, too close: disturbed flow)

Competitive flow: In case native coronary is not snared and competitive flow is suspected, repeat measurement with (manually) occluded native coronary, use measurement with highest Q_{mean}

Negative or near-zero flow: Absolute flow rate is used for DF%, D/S-ratio, to avoid negative or near-infinite values

The rationale of deploying Q_{mean} as a patency metric is simply that in a narrowed anastomosis the resistance to flow is greater (Figure 2), leading to a reduction of Q_{mean} . However, Q_{mean} is also influenced by other factors like graft diameter, autoregulation, driving pressure gradient, competitive flow, and quality of distal run-off, which makes it an unreliable metric if used on its own.

PI quantifies flow pulsatility relative to mean flow rate, which tends to increase with increasing occlusion. This is mostly an effect of graft compliance [18] and thus depends on flow probe position. Also, the negative systolic spike caused by competitive flow leads to elevated PI, irrespective of graft quality.

DF% and D/S-ratio, which are related as $DF\% = 100 \times D/S\text{-ratio}/(1 + D/S\text{-ratio})$, quantify diastolic dominance of the graft flow waveform by comparing volume delivered during diastole with per-beat volume or systolic volume, respectively. An analogous metric, Diastolic-Systolic Velocity Ratio, was recently introduced to quantify stenosis in the catheterization laboratory [19]. With increasing graft occlusion, the diastolic dominance of the flow waveform decreases (Figure 3). This is, at least in part, explained by the pressure-dependent resistance in the myocardium: a decrease in pressure leads to an increase in resistance [12]. Because the pressure drop over a stenosis depends on the flow rate through the stenosis, this effect will be more pronounced during diastole. As a result, the flow rate is affected more severely by stenosis during diastole than during systole. Furthermore, stenosis induces autoregulation, which reduces the subendocardial/subepicardial flow ratio [12]. As a result, a larger portion of the flow passes through the subepicardium where flow impediment due to systolic contraction is not as strong as in the subendocardium.

Critical values of DF% and D/S-ratio depend on graft target site and flow probe position. Finally, also the amount of retrograde graft flow is sometimes displayed on flow monitors. Called insufficiency ratio, or backflow percentage, it is quantified by the ratio (negative flow volume)/(total flow volume). While retrograde flow may cause string sign in the graft and eventual failure, it is not an indicator of technical error in the graft or anastomosis [1].

Flow-based CABG patency evaluation:

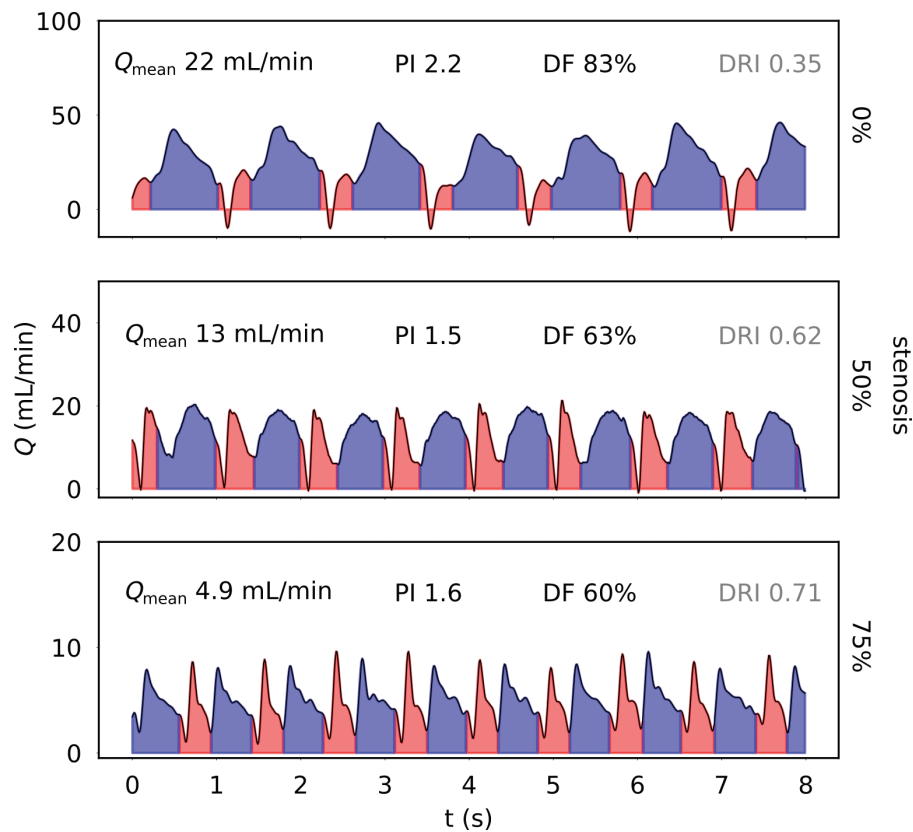


Figure 3: Diastolic dominance of coronary flow waveform decreases with increasing occlusion (representative flow waveforms courtesy of Takahashi et al., Nippon Medical School, Tokyo, Japan)

2.3 Recent Developments

Research into improved TTFM-based patency metrics is ongoing. Epicardial ultrasound imaging is sometimes used to inspect the distal anastomosis interior and is considered a useful complement to TTFM [1, 4].

Takami and Ina [20] proposed to use the Fast Fourier Transform (FFT), more specifically, the ratio of powers of the fundamental frequency and its first harmonic. Jia et al. [21] tested this idea and extended it to a number of other FFT-related metrics in a clinical study.

Handa et al. [22] introduced the maximal blood flow acceleration in early diastole as a potential marker of patency.

Furthermore, combining multiple metrics and applying machine learning techniques, such as neural networks [23] or support vector machines [24], can potentially improve the accuracy of flow-based intraoperative patency assessment, albeit at the cost of increased mathematical complexity and reduced explainability.

Finally, in the related setting of diagnostic cardiac catheterization laboratory measurements, deMarchi et al. [25] attempted to use coronary wave intensity analysis [26] to determine stenosis severity from flow and pressure measured proximal to a coronary stenosis, but failed to find a statistically significant relation.

2.4 Diastolic Resistance Index

For a more complete metric, with a more conceptually tangible link to graft patency, Transonic is working on the development of a novel metric — the diastolic resistance index (DRI):

$$\text{DRI} = \frac{\bar{p}_{\text{dia}}/\bar{Q}_{\text{dia}}}{\bar{p}_{\text{sys}}/\bar{Q}_{\text{sys}}}$$

Like DF% and D/Sratio, DRI compares diastolic and systolic flow rates, and will therefore quantify the decrease of diastolic dominance with increasing occlusion. Because DRI uses mean flow rates rather than volumes, it is expected to be less sensitive to diastolic time fraction. The influence of perfusion pressure is taken into account by including the ratio of mean diastolic to mean systolic pressure. Central pressure

physical & statistical background cont.

is estimated from peripheral measurements using a transfer function [13]. With increasing anastomotic occlusion, resistance increases, and so does DRI, rendering it more intuitive than DF% or D/S-ratio.

3. Performance Assessment

To evaluate how well a particular patency metric performs in practice, results from a clinical study are analyzed statistically. Conventionally, binary classification is used for CABG patency metrics. That is, depending on the value of a metric, a graft is considered either patent or failed. The class predicted by the metric is then compared with the 'true' class, based on a gold-standard measurement method, such as angiography. In the case of binary classification, four different outcomes are possible, as shown in Table 2.

Table 1: Possible outcomes in binary classification. TN: true negative, FN: false negative, FP: false positive, TP: true positive

| | | actual | |
|-----------|--------|--------|--------|
| | | patent | failed |
| predicted | patent | TN | FN |
| | failed | FP | TP |

Doing this for a sufficiently large number of grafts, the true positive rate, or sensitivity, and the true negative rate, or specificity, can be determined. Sensitivity and specificity depend on the threshold value selected for a metric. For example, if the threshold for Q_{mean} is set to a relatively high value (i.e. all grafts with $Q_{\text{mean}} < 25$ mL/min are labeled as failed), the sensitivity will be very high, but there will also be a lot of false positives (i.e. patent grafts that are incorrectly labeled as failed), resulting in a low specificity. To find the optimal balance between sensitivity and specificity, a so-called receiver operating characteristic (ROC) curve can be constructed. The threshold is varied over the entire range of values measured in the study, and for each value the sensitivity and specificity are determined. This results in a curve that runs from 0% sensitivity, 100% specificity, to 100% sensitivity, 0% specificity (see example in Figure 4). The area under this curve is a measure of the performance of a metric: an area of 1.0 means perfect performance, while an area of 0.5 indicates pure chance; the worst possible performance.

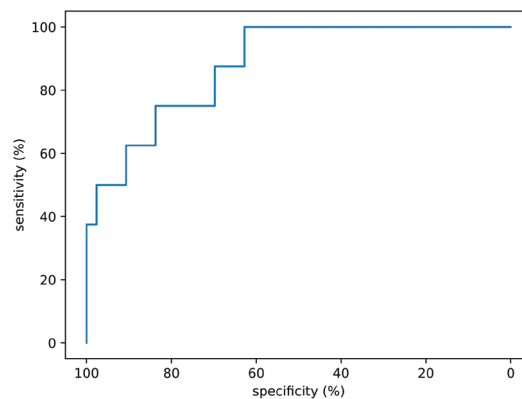


Figure 4: Example of an ROC curve (based on mean flow rate data from a pig study by Morota et al. [27])

Flow-based CABG patency evaluation:

3.1 Three-class Statistics

A disadvantage of binary classification is that it doesn't indicate the severity of a detected occlusion; a graft can only be patent or failed. Still, a surgeon's decision to revise a graft depends on many factors, and in some cases may be influenced by the severity of a possible occlusion as suggested by TTFM. Therefore, Transonic is testing a more elaborate method, moving away from the conventional binary classification framework, to accommodate the use of three instead of two graft quality grades: patent, subcritical stenosis, and critical stenosis. Using multi-class statistics enables direct quantification of the ability of a metric (i.e. Q_{mean} , PI, DF%, DRI) to correctly place a new measurement in one of these three categories, rather than comparing categories one vs. one, or one vs. rest, as is done when using binary methods. Because, to the best of our knowledge, such a multi-class analysis is new to the field of CABG patency evaluation, a detailed explanation is given here of the Bayesian multi-class approach that was used in our retrospective analysis. This explanation is based on papers by Brodersen et al. [28], Carrillo et al. [29] and Kautz et al. [30].

Graft patency evaluation can be considered a decision problem, in which each graft is associated with a class label from a finite set of categories. In our case, three categories were used, but the method is equally applicable to different numbers of categories. For example, if applied with two categories, it would be the Bayesian extension of the familiar binary classification performance evaluation, as it is conventionally applied in the evaluation of indicator performance.

In the following, the graft flow measurements, and the metric values computed based on these measurements, are assumed to be independent and identically distributed (i.i.d.). The goal of the analysis is to quantify the ability of a metric to predicting the correct category on future measurement data, based on the presently available classification results. That is, we wish to estimate the performance of a metric, and express it as a number $\lambda \in [0, 1]$, where 0 means that the metric is most likely to give incorrect results in all future instances, and 1 means that it is expected to correctly predict the category in all future instances. Two important differences between Bayesian and frequentist statistics are that, first, the performance λ is considered to be a latent (i.e. unobservable) variable, and second, instead of a point estimate, a posterior probability distribution of λ is computed. Starting from a prior distribution $p(\lambda)$, a posterior distribution is computed, conditioned on observed data: $p(\lambda|\mathcal{D})$.

3.1.1 Bayesian Inference

Based on the value of a metric, a graft is assigned a category. This classification result can either be correct or incorrect, denoted as $y = 1$ or $y = 0$, respectively, so that a sequence of outcomes y_1, \dots, y_n is obtained. These outcomes can be considered as the i.i.d. result of a Bernoulli experiment¹:

$$p(y_i|\lambda) = \text{Bern}(y_i|\lambda) = \lambda^{y_i}(1-\lambda)^{(1-y_i)}, \quad (1)$$

where, as explained earlier, λ is the (unknown) probability of any one trial being classified correctly. This means that the number of correct predictions k in our sequence of n outcomes ($k \leq n$) follows a binomial distribution²:

$$p(k|\lambda, n) = \text{Bin}(k, \lambda, n) = \binom{n}{k} \lambda^k (1-\lambda)^{n-k}. \quad (2)$$

To proceed, a prior on λ needs to be chosen, to express any available prior knowledge about classification performance. A natural choice for this is the Beta distribution, which is the conjugate prior of the binomial distribution. Because generally, previous classification results are not available, it is common practice to choose a so-called uninformed prior. This gives a uniform distribution, in which every value for $\lambda \in [0, 1]$ is considered equally likely:

$$p(\lambda) = \text{Beta}(\lambda|1, 1) \quad (3)$$

(of course, if previous results were available, the prior could be adjusted based on these). Now, based on the observed n grafts with k correct predictions, the posterior distribution can be computed as:

$$p(\lambda|k, n) = \frac{\text{Bin}(\lambda|k, n) \times \text{Beta}(\lambda|1, 1)}{p(k)} = \text{Beta}(\lambda|k+1, n-k+1). \quad (4)$$

1. Bernoulli experiment: experiment with either success or failure as outcome, i.e. a prediction is either correct, with probability λ , or incorrect, with probability $(1-\lambda)$.
2. Binomial distribution: discrete probability distribution of the number of successes in a sequence of n independent Bernoulli experiments.

physical & statistical background cont.

3.1.2 Application in Multi-class Setting

If our data were perfectly balanced, that is, if we would have a dataset with equal numbers of patent, sub-critical and critical grafts, equation (4) could be used directly to obtain an estimate of classification performance:

$$p(\lambda|k, n, a, b) = \text{Beta}(\lambda|a + k, b + n - k). \quad (5)$$

The mode of this posterior distribution minimizes the expected loss of a (0, 1)-loss function:

$$\text{mode} = \frac{k + a - 1}{a + b + n - 2}. \quad (6)$$

Starting from an uninformed prior, with $a = b = 1$, this mode equals the conventional sample accuracy, or sensitivity, k/n .

However, often measured data is not perfectly balanced. Typically, in a clinical setting, the number of patent grafts is far higher than the number of critically stenosed grafts. In such cases, using the sample sensitivity may give misleading results. If, for example, in a binary classification setting, a set of 100 grafts contained 5 patent and 95 failed grafts (not a very likely scenario, admittedly), even a classifier that trivially labeled all grafts as failed would achieve a sensitivity of 0.95, or 95%. In reality, this trivial classifier should be assigned a sensitivity of 0.5, or 50% (pure chance), and likewise, the minimum sensitivity in a setting with l classes is $1/l$. In binary classification, this problem is circumvented by also reporting the specificity, which essentially represents the sensitivity for the patent class. By constructing the receiver operating characteristic (ROC) curve, the sensitivity and corresponding specificity for a range of metric cut-off values are visualized. The area under this curve is a measure for the performance of a metric, where a value of 1 represents perfect performance, and a value of 0.5 corresponds to pure chance.

Another way of resolving this issue, which is more straightforward to carry over to a multi-class setting, is to use the balanced sensitivity, that is, the arithmetic mean of the class-wise sensitivities. Using the arithmetic mean “as is” implies that equal weight is assigned to each class. If the cost of misclassification for a particular class is deemed higher than for others (e.g. incorrectly evaluating a stenosed graft as patent may be considered as a more serious error than incorrectly evaluating a patent graft as stenosed), a weighted arithmetic mean can be used instead.

The equivalent of the arithmetic mean for probability distributions is convolution. After computing the posterior Beta distribution for each class, the convolution of these distributions gives the posterior distribution for the balanced sensitivity (computationally, it is often more efficient to work in the Fourier domain to achieve this). In our work, the mode of the resulting distribution is reported as the posterior balanced sensitivity (PBS).

3.1.3. Implementation

As described earlier, a graft is assigned to one of the pre-defined categories, based on the value of a metric. Generally, this is done using logistic regression, but other classification methods, like a decision tree classifier may also be used. In any case, correction for class imbalance is desirable. Ideally, the available dataset is divided into a training set and a test set, or (stratified) k -fold cross validation is used. However, in the setting of CABG patency evaluation datasets are typically too small for one of these strategies to be feasible, and the complete dataset tends to be used directly. In itself, this does not necessarily pose a problem, but it should be kept in mind that this introduces the risk of overfitting (i.e. bad generalizability).

Similar to the binary classification case (Table 1), the results of this classification can be conveniently represented in a so-called confusion matrix: the rows of this matrix represent the predicted category, while the columns indicate the true category. As an example, the confusion matrix for Q_{mean} applied to the pig data of Morota et al. [27] is shown in Table 2.

Flow-based CABG patency evaluation:

Table 2: Confusion matrix for Q_{mean} applied to the pig data of Morota et al. [27]

| | | actual | | |
|-----------|--------------|--------|--------------|----------|
| | | patent | sub-critical | critical |
| predicted | patent | 9 | 3 | 1 |
| | sub-critical | 7 | 3 | 3 |
| | critical | 0 | 2 | 23 |

The numbers in the columns sum to the total number of grafts in that class. For example, the pig data contains 16 patent grafts, 9 of which were (correctly) predicted to be patent based on Q_{mean} , and 7 were (incorrectly) predicted to be sub-critically stenosed. From the confusion matrix, the number of true positive predictions (tp_m) for each class m is the number on the corresponding diagonal, while the number of false negative predictions (fn_m) is the sum of the remaining numbers in the m^{th} column:

$$tp_m = c_{m,m}, \quad fn_m = \sum_{i=1, i \neq m}^k c_{i,m}, \quad (7)$$

where k is the number of classes, or categories.

When an uninformed prior is used, with $a = b = 1$, the parameters for the posterior Beta distribution for class m can be determined from tp_m and fn_m :

$$a_m = tp_m + 1, \quad b_m = fn_m + 1. \quad (8)$$

After all class-wise posterior distributions have been computed, the posterior balanced sensitivity distribution is obtained as the convolution of these class-wise distributions (Figure 4).

The mode of this distribution is reported as the posterior balanced sensitivity (PBS), to express the overall performance of a metric, while the modes of the class-wise probability distributions are also reported, to provide insight into the strong and weak points of that particular metric.

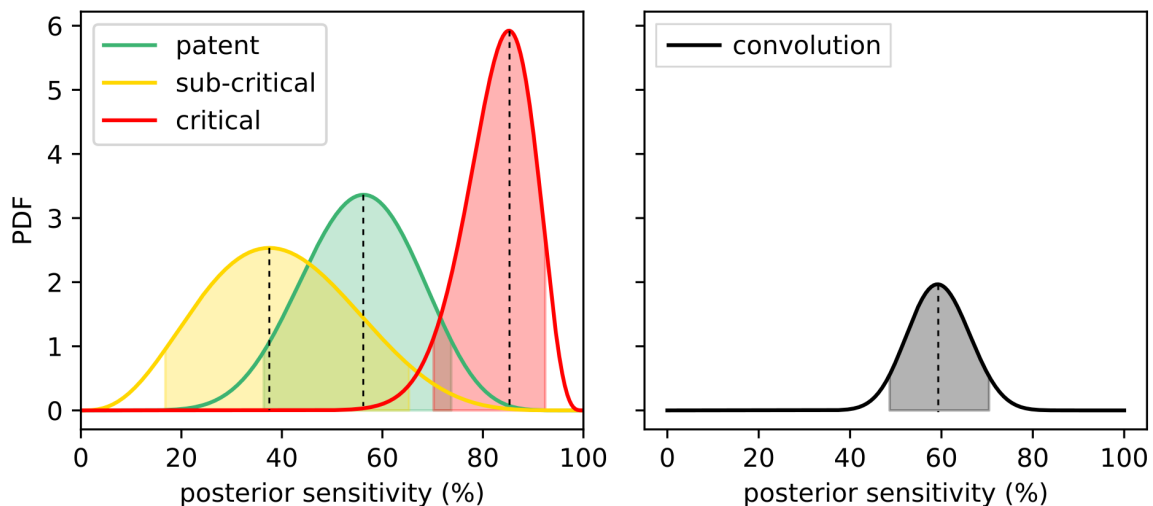


Figure 5. Left: Class-wise posterior probability distributions for sensitivity of Q_{mean} right: result of convolution, posterior balanced sensitivity of Q_{mean} . Dashed vertical lines indicate modes, shaded areas indicate 95% confidence intervals.

physical & statistical background cont.

Abbreviations

| | |
|-----------|--------------------------------------|
| BF% | backflow percentage |
| BMI | body mass index |
| C | compliance |
| CABG | coronary artery bypass graft |
| D | diameter |
| DF% | diastolic filling percentage |
| DRI | diastolic resistance index |
| D/S-ratio | diastolic/systolic ratio |
| FFT | fast Fourier transform |
| LITA | left internal thoracic artery |
| LAD | left anterior descending artery |
| p | pressure, probability (from context) |
| PBS | posterior balanced sensitivity |
| PI | pulsatility index |
| Q | flow rate |
| R | resistance |
| ROC | receiver operating characteristic |
| t | time |
| T | cardiac period |
| TTFM | transit-time flow measurement |
| V | volume |

Subscripts

| | |
|----------------|------------------------|
| dia, sys | diastole, systole |
| min, max, mean | minimum, maximum, mean |

Flow-based CABG patency evaluation: physical and statistical background

References

1. Akhrass R, Bakaeen FG. Intraoperative graft patency validation: Friend or foe? *JTCVS Tech*. 2021 Jan 6;7:131-137.
2. Head SJ, Kieser TM, Falk V, Huysmans HA, Kappetein AP. Coronary artery bypass grafting: Part 1--the evolution over the first 50 years. *Eur Heart J*. 2013 Oct;34(37):2862-72.
3. Head SJ, Börgermann J, Osnabrugge RL, Kieser TM, Falk V, Taggart DP, Puskas JD, Gummert JF, Kappetein AP. Coronary artery bypass grafting: Part 2--optimizing outcomes and future prospects. *Eur Heart J*. 2013 Oct;34(37):2873-86.
4. Taggart DP, Thuijs DJFM, Di Giammarco G, Puskas JD, Wendt D, Trachiotis GD, Kieser TM, Kappetein AP, Head SJ. Intraoperative transit-time flow measurement and high-frequency ultrasound assessment in coronary artery bypass grafting. *J Thorac Cardiovasc Surg*. 2020 Apr;159(4):1283-1292.e2.
5. Thuijs DJFM, Bekker MWA, Taggart DP, Kappetein AP, Kieser TM, Wendt D, Di Giammarco G, et al. Improving coronary artery bypass grafting: a systematic review and meta-analysis on the impact of adopting transit-time flow measurement. *Eur J Cardiothorac Surg*. 2019 Oct 1;56(4):654-66
6. Sandner SE, Gaudino MFL. Commentary: Transit time flow measurements for coronary artery bypass graft: Go with the flow. *JTCVS Tech*. 2020 Dec 26;7:144-145.
7. Bozinovski J. Commentary: Measure twice, cut as directed--Transit-time flow measurement and high-frequency ultrasound-guided surgical revision. *J Thorac Cardiovasc Surg*. 2020 Apr;159(4):1293-1294.
8. Paone G. Commentary: Is routine use of transit-time flow measurement and high frequency ultrasound assessment in coronary bypass grafting ready for prime time, or a waste of time? *J Thorac Cardiovasc Surg*. 2020 Apr;159(4):1295-1296.
9. Kim KB, Choi JW, Oh SJ, Hwang HY, Kim JS, Choi JS, Lim C. Twenty-Year Experience With Off-Pump Coronary Artery Bypass Grafting and Early Postoperative Angiography. *Ann Thorac Surg*. 2020 Apr;109(4):1112-1119.
10. Nakamura M, Yaku H, Ako J, Arai H, Asai T, et al. Japanese Circulation Society Joint Working Group. JCS/JSCVS 2018 Guideline on Revascularization of Stable Coronary Artery Disease. *Circ J*. 2022 Feb 25;86(3):477-588.
11. Sousa-Uva M, Neumann F-J, Ahlsson A, Alfonso F, Banning AP, Benedetto U et al. 2018 ESC/EACTS guidelines on myocardial revascularization. *Eur J Cardiothorac Surg* 2019; 55:4-90.
12. Spaan JAE, Piek JJ, Siebes M. Coronary circulation and hemodynamics. In: Sperelakis N, Kurachi Y, Terzic A, Cohen MV, editors. *Heart physiology and pathophysiology*. Fourth edition, 2001.
13. Nichols WW, O'Rourke MF, Vlachopoulos C. McDonald's *Blood Flow in Arteries - Theoretical, Experimental and Clinical Principles*. 6th ed. Hodder Arnold; 2011.
14. Lee SW, Jo JY, Kim WJ, Choi DK, Choi IC. Patient and haemodynamic factors affecting intraoperative graft flow during coronary artery bypass grafting: an observational pilot study. *Sci Rep*. 2020 Jul 31;10(1):12968.
15. Mantero S, Pietrabissa R, Fumero R. The coronary bed and its role in the cardiovascular system: a review and an introductory single-branch model. *J Biomed Eng*. 1992 Mar;14(2):109-16.
16. Tedoriya T, Kawasuji M, Sakakibara N, Ueyama K, Watanabe Y. Pressure characteristics in arterial grafts for coronary bypass surgery. *Cardiovasc Surg*. 1995 Aug;3(4):381-5.
17. Young DF, Tsai FY. Flow characteristics in models of arterial stenoses. II. Unsteady flow. *J Biomech*. 1973 Sep;6(5):547-59.
18. Jelenc M, Jelenc B, Klokocovnik T, Lakic N, Geršak B, Knežević I. Understanding coronary artery bypass transit time flow curves: role of bypass graft compliance. *Interact Cardiovasc Thorac Surg*. 2014 Feb;18(2):164-8.
19. Waard GA, Broyd CJ, Cook CM, van der Hoeven NW, Petraco R, Nijjer SS, et al. Diastolic-systolic velocity ratio to detect coronary stenoses under physiological resting conditions: a mechanistic study. *Open Heart*. 2019 Mar 1;6(1):e000968
20. Takami Y, Ina H. A simple method to determine anastomotic quality of coronary artery bypass grafting in the operating room. *Cardiovasc Surg*. 2001 Oct;9(5):499-503.
21. Jia Y, Xu H, Su P, Gao J, Gu S, Liu Y, An X, Yan J, Zhang X. Predictive value of graft patency and major adverse cardiac and cerebrovascular events (MACCEs) in coronary artery bypass grafting (CABG) based on Fourier transform (FFT). *J Thorac Dis*. 2021 May;13(5):2705-2715.
22. Handa T, Orihashi K, Nishimori H, Fukutomi T, Yamamoto M, Kondo N, Tashiro M. Maximal blood flow acceleration analysis in the early diastolic phase for in situ internal thoracic artery bypass grafts: a new transit-time flow measurement predictor of graft failure following coronary artery bypass grafting. *Interact Cardiovasc Thorac Surg*. 2015 Apr;20(4):449-57.
23. Cerrito PB, Koenig SC, VanHimbergen DJ, Jaber SF, Ewert DL, Spence PA. Neural network pattern recognition analysis of graft flow characteristics improves intra-operative anastomotic error detection in minimally invasive CABG. *Eur J Cardiothorac Surg*. 1999 Jul;16(1):88-93.
24. Mao B, Feng Y, Wang W, Li B, Zhao Z, Zhang X, Jin C, Wu D, Liu Y. The influence of hemodynamics on graft patency prediction model based on support vector machine. *J Biomech*. 2020 Jan 2;98:109426.
25. deMarchi SF, Gassmann C, Traupe T, Gloekler S, Cook S, Vogel R, Gysi K, Seiler C. Coronary wave intensity patterns in stable coronary artery disease: influence of stenosis severity and collateral circulation. *Open Heart*. 2019 Oct 23;6(2):e000999.
26. Davies JE, Whinnett ZI, Francis DP, Manisty CH, Aguado-Sierra J, et al. Evidence of a dominant backward-propagating "suction" wave responsible for diastolic coronary filling in humans, attenuated in left ventricular hypertrophy. *Circulation*. 2006 Apr 11;113(14):1768-78.
27. Morota T, Duhaylongsod FG, Burfeind WR, Huang CT. Intraoperative evaluation of coronary anastomosis by transit-time ultrasonic flow measurement. *Ann Thorac Surg*. 2002 May;73(5):1446-50.
28. Brodersen, KH, Ong, CS, Stephan, KE, Buhmann, JM. The balanced accuracy and its posterior distribution. In: *International Conference on Pattern Recognition* 2010.
29. Carrillo H, Brodersen KH, Castellanos JA. Probabilistic performance evaluation for multiclass classification using the posterior balanced accuracy. In: *ROBOT2013: First Iberian Robotics Conference* 2014;347-361.
30. Kautz T, Eskofier BM, Pasluosta CF. Generic performance measure for multiclass-classifiers. *Pattern Recognit* 2017;68:111-125.